

A sensor for confident identification of structural damage in reinforced concrete buildings

Mete A. Sözen^{1*} and Santiago Pujol²

¹*Department of Structural Engineering, Purdue University, West Lafayette, IN 47905, USA*

²*Department of Civil Engineering, Purdue University, West Lafayette, IN 47905, USA*

(Received July 19, 2008, Accepted July 1, 2009)

Abstract. A specific type of structural damage that would benefit from remote sensing is discussed and a solution is suggested.

Keywords: sensor; structural assessment; reinforced concrete; damage; detection; wireless.

1. Introduction

This paper has been written from the viewpoint of need. Its goal is not to provide a final solution but to suggest, within a limited segment of the construction industry, where there is a need and suggest where there may be a solution. From their recent experiences, it appears to the writers that there are needs and there exist solutions, but the two seldom intersect, possibly because of lack of communication among professions.

Before getting into detail, we start with a case that we find loud and clear. Had there been a handful of temperature sensors in the World Trade Center buildings on 11 September 2001 and had there been a system to have them read remotely, much of the tragedy could have been avoided. Even though there have been many imaginative explanations of the collapse of the World Trade Center Towers in the technical and popular press, by now most engineers have understood that the critical event in the collapses was the loss of fire insulation during aircraft impact. Once the insulation was lost substantially and once the metal temperature exceeded 650 °C, the steel structures did not have much of a chance for survival. In fact, collapse would have occurred even if there had been no structural damage resulting from the impact. Had the temperature sensors been there, as a minimum the firefighters' lives could have been spared.

We start with this simple and naïve example primarily to emphasize that there may be many applications well within our current technology that may turn out to be very useful for society, but it is not easy to get the various groups involved in the decisions to understand the risks and the solution possibilities. In that respect, the situation is not much different from that of seat belts in cars in the 1960's. What was considered to be an unusual and unnecessary expense then, has been for some time considered to be a natural requirement in an automobile. Seat belts were available

*Corresponding Author, Kettelhut Distinguished Professor, E-mail: sozen@purdue.edu

before the 1960's and the dangers were there well before the 1960's. But the sensitivity and the knowledge were not there. At the beginning of the 21st century, there are dozens of needs for sensors as well as, we suspect, currently available solutions, but those who understand the needs may not be in communication with those who may have the solutions.

In this paper, we focus on a simple solution for identifying critical earthquake damage in reinforced concrete buildings. We believe that the need exists as does the solution. The challenge is in convincing the building industry in seismic regions to appreciate the need and for those in sensor technology to package the solution. We say "package" because we believe the required components are extant.

The need is very simply explained. After a major earthquake in a region with aging construction, there may be a considerable number of buildings that are still standing up but have been critically damaged. An aftershock or even simply time may cause collapse. Such buildings need to be identified as soon as possible. The best solution is naturally to have the requisite number of experienced experts to be rushed to the region. Unfortunately, not every region is blessed with the requisite number of experts. Correct identification takes days or even months. A simple solution is to have sensor systems to enable a quick "up or down" evaluation by remote sensing.

2. Holiday inn, Van Nuys, California

The seven-story Holiday Inn Building (Fig. 1) was built in 1966. Figs. 2 and 3 show the plan and an elevation of the reinforced concrete structure. The reinforced concrete frames along the boundaries of the structure were built to resist the lateral forces induced by earthquakes. The footprint of the structure measured approximately 66 ft (N-S) by 150 ft (E-W). The height of the main structure was approximately 66 ft.

The building suffered light damage in the San Fernando earthquake of 1971. At that time, only three sensors had been mounted on the structure. After the 1971 event, the building was equipped with 16 accelerometers installed at locations indicated in Fig. 4(CDMG 1994), during the Northridge earthquake, the damage was serious but the structure did not collapse. The peak ground acceleration



Fig. 1 Holiday inn building, Van Nuys, CA

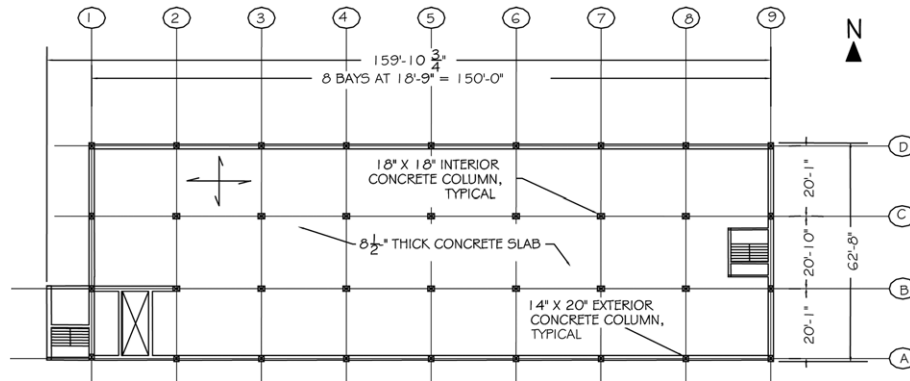


Fig. 2 Typical floor framing plan, holiday inn building

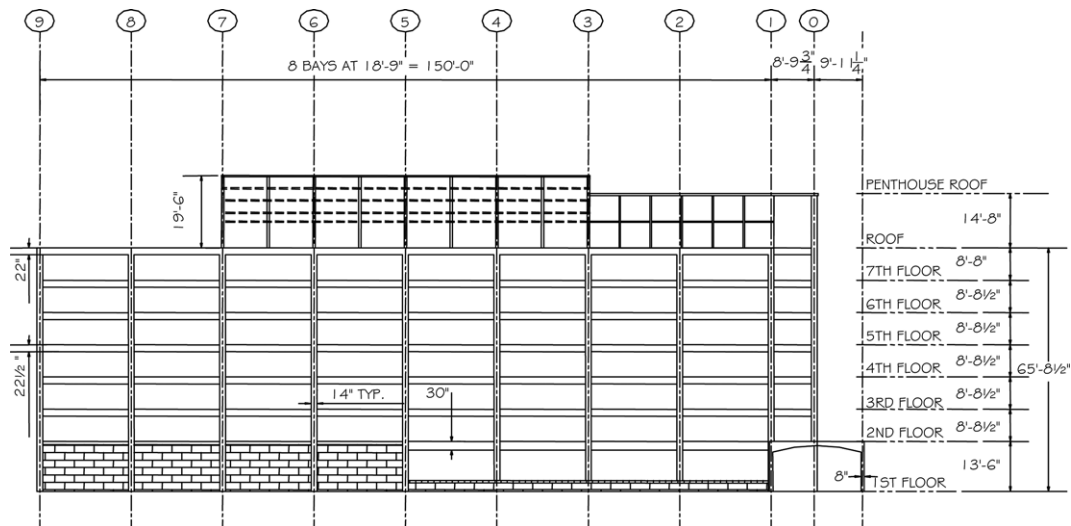


Fig. 3 North perimeter frame elevation

measured in the basement of the structure was 0.25 g in 1971. In 1994, it was 0.44 g.

First, we ask whether we could infer the level of the damage caused by the Northridge Earthquake from the output of the accelerometers. The direct answer to that question is best found in the measured story distortions. Assuming that the integration of the acceleration data to develop displacement data was without fault, we examine the drift responses in Fig. 5 through 7.

The mean drift ratio (ratio of roof lateral displacement to the height above base) history in Fig. 5 suggests that the effective period of the structure during strong motion was approximately 2 sec. Compared with the estimated initial lowest-mode period of 1.2 sec. the observation does not cause alarm. A reduction in effective stiffness to approximately 1/4 of calculated stiffness based on uncracked sections is not abnormal. And a maximum mean drift ratio of approximately 1% is not an unequivocal indicator of serious CA. damage. Thinking of a frame with reasonably uniform stiffness and mass distribution, it is expected that the story drift ratios in the lower stories would be higher approximately by 50%.

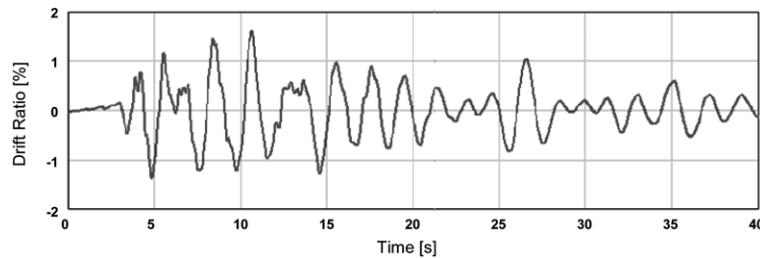


Fig. 7 Drift ratio, story 2, North-South, 1994 Northridge earthquake

it was not possible to sense the critical damage to the framing from acceleration data. And this is not difficult to understand because, in a structure with many structural elements, failure of a few is not likely to be reflected in acceleration and certainly not in displacement records.

It would not be correct to assume from one experience that a certain device will not produce the results needed. But in the case of the Holiday Inn Van Nuys building, the reason for the lack of evidence in the acceleration records can be understood in terms of the overall phenomena of response.

That was the primary reason that drove us to seek another solution.

The disadvantage of concrete, that it cracks at service loads, is in this respect an advantage. Because it gives us a way to understand what happened and what may yet happen. Inspired by the work by Wood and Neikirk (2001), Morita and Noguchi (2006), we decided to develop a sensing system that would provide a categorical “up or down” indication of critical damage in a reinforced concrete structure. We sought a sensor-communication system having the following characteristics with the assumption that the placement of the sensor would be determined correctly by an expert.

- A sensor that would discriminate between the usual service-load cracks and cracks critical to the safety of the structure.
- A sensor that can be manufactured using inexpensive off-the-shelf components
- A sensor query system consisting of low-cost open data and communication protocols.
- A sensor query system that would allow clutter-free installation.
- A sensor query system that would be flexible enough to incorporate new developments in sensing and data acquisition.
- A sensor query system with wireless communication.

3. Design of the proposed sensor

The driving criteria in the design of the sensor were simplicity of its manufacture, its ruggedness, and its ability to discriminate crack width. A very simple arrangement, shown in Fig. 8 was selected. The sensor consisted of a conducting unit formed by joining two strips of steel with a thin strip of copper. The copper strip was made using GC Tool Pure Copper Circuit Tape having a width of 1/8 in. and a thickness of 0.002 in. Each steel strip had a length $L_s/2$ and measured 3/8 in. in width and 0.005-in. in thickness. In the applications discussed in this paper, L_s was 16 in. Each end of the sensor is attached to the structure to be monitored while the segment of the sensor between the attachment points remains free. Deformations and cracks occurring in the structure between the attachment points can cause large strains in the copper strip. Depending on the length L_c , a given

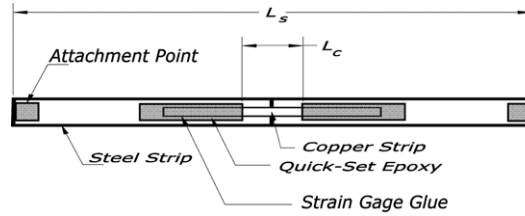


Fig. 8 Proposed sensor

deformation between attachment points can cause the copper strip to break, signaling that the structure may have reached a critical stage. Length L_c determines the sensitivity of the sensor to deformations and cracks occurring along length L_s . The length L_s can be adjusted to increase or decrease the size of the area being monitored.

4. Data acquisition and communication

The proposed sensor was tested in a rapid structural assessment network (RSAN). In this network, data collected at the sensors are transported over a multihop wireless network to a set of Internet connected access points (APs). The network was designed to allow a complex of sensors in many buildings to be monitored by a single remote-control center. Three options were considered to monitor the sensors:

1. Passive RFID,
2. MDA320CA analog/digital data acquisition boards working with CrossbowMICA2 motes, and
3. High-precision ADAM-6017 acquisition modules working with 802.11 routers.

4.1 Passive RFID

The crack-width sensor can be embedded in a passive RFID tag, so that its status can be queried by a nearby RFID reader. The RFID tag consists of an antenna loop and a small integrated circuit containing a small amount of information (e.g., an ID associated with the location of the sensor in

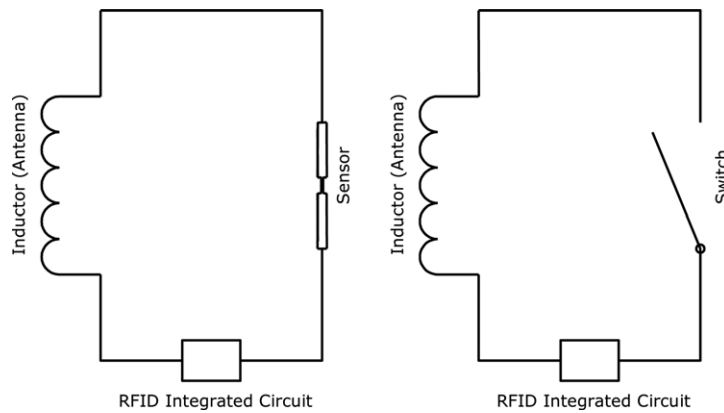


Fig. 9 Integration of the proposed sensor in an RFID tag

the structure), which is transmitted from tag to reader when the tag is excited by the reader. The tag reflects energy from the reader and requires no power to operate. The sensor is embedded as part of the antenna loop as shown in Fig. 9. The sensor acts as a switch in the antenna loop that opens if the sensor ruptures as the substrate deforms and cracks.

Passive RFID tags are quite inexpensive and can be produced for approximately one dollar per tag. RFID readers are more expensive. Lower-end readers have a unit price of approximately \$50 if bought in dozens. However, a single instrument can be used to query a number tags reducing the reading-instrument cost per sensor. In our implementation, we used RFID readers/tags manufactured by Phidgets (2008). The Phidgets reader generates a reading of the tag ID whenever a tag comes in or out of range. A reader placed near a tag will detect the tag until the sensor embedded in the tag ruptures. At that time, the RFID reader will report the loss of connection with the tag, identifying the occurrence of deformations exceeding the selected crack-width threshold.

The Phidgets reader used has a limited reading range (less than one foot) and cannot query tags within this range selectively. Readers placed closely (the distance between them not exceeding one metre) will interfere with one another. We used one reader per tag to simplify the experiments we ran, raising the installation cost (from an achievable few dollars per sensor to approximately \$50/sensor). The cost was a limitation of our current experimental hardware, and is not a limitation of passive RFID technology. The cost can be reduced connecting several sensors in series within the antenna loop.

The Phidgets reader has a USB interface for communication. To connect multiple readers to the network at low cost, we used a Keyspan US-4A USB server (unit cost of approximately \$100). The server was connected to an Ethernet interface that provided connectivity with a Linksys 802.11 router. The router provides wireless connectivity to a set of Internet-enabled AP's using TCP/IP. The arrangement of the system is shown schematically in Fig. 10.

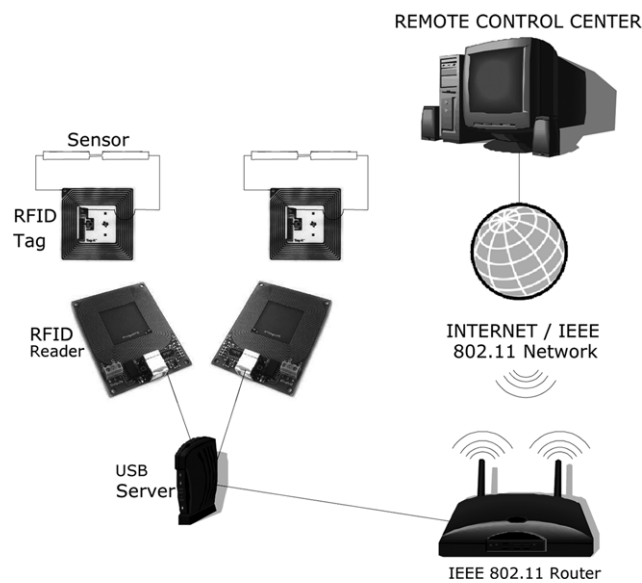


Fig. 10 System used to read RFID tags remotely

4.2 Mote-based data acquisition/communication

There is a wide range of wireless platforms that can support sensors to monitor structures (Straser and Kiremidjian 1998, Lynch *et al.* 2001, Wang *et al.* 2005, Aoki *et al.* 2003, Farrar *et al.* 2005, Chung *et al.* 2004, Zhao and Guibas 2004, Crossbow Technology 2009). We used Crossbow MICA2 motes to query the status of crack-width sensors by connecting an MDA320CA data acquisition board to a MICA2 processor/radio module. The MDA320CA data acquisition board has eight 16-bit channels for single-ended 0.0-2.5 V ADC inputs and eight digital I/O channels. It also provides 2.5 V excitation output for sensors. In our application, we connected a number of sensors to the analog and the digital channels of the data-acquisition board. Fig. 11(a) shows the wiring of four sensors to the single-ended voltage ADC inputs of the board.

The E2.5 terminal denotes the 2.5 V excitation channel on the circuit board. This terminal is connected to one end of each sensor. The other end of the sensor is connected to the input of an ADC channel and to an array of 10-k pull-down resistors. The pull-down resistors are used to prevent the ADC inputs from staying in a floating state. In that state, the voltage is unknown and is vulnerable to environmental interference. This wiring arrangement produces a 2.5 V reading if the copper strip retains its original length and 0V if the copper strip is broken. In an intermediate state in which the strip is strained but not broken, the reading remains close to 2.5V. Fig. 11(b) shows the wiring of the sensors to the digital channels. The wiring connects one end of the sensor to the digital input and the other end to an electrical ground. The wiring produces a low reading (GND) if the copper strip is not broken (because the sensor closes the circuit to GND), and a high reading if the strip is broken.

The MDA320CA collects data from a set of sensors, each of which is connected through a separate data channel. The MICA2 mote connected to the MDA320CA can then relay the collected data over a 900 MHz radio-frequency (RF) channel to other RF devices. In our application, we used other motes as the wireless relay nodes to communicate the sensor data through an RF/Ethernet gateway to the Internet. The gateway, which was named the *mote-network gateway*, forwards data between a group of local MICA2 mote systems and the Internet-accessible remote control center. The setup is shown schematically in Fig. 12.

A MICA2 mote has a unit price of approximately \$100 and an MDA320CA data acquisition board has a unit price of approximately \$200. The combined hardware costs six times as much as a

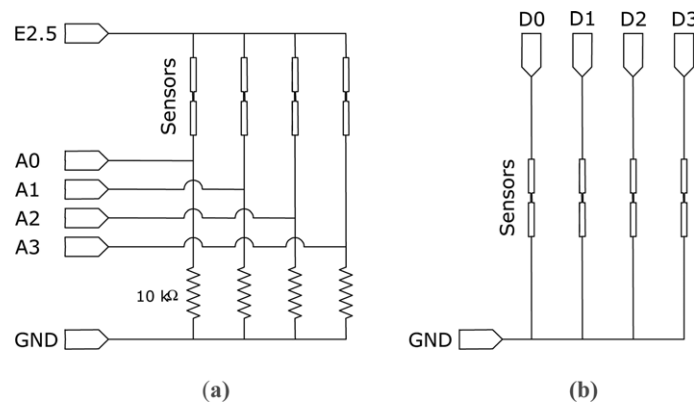


Fig. 11 Connections to MDA320CA board

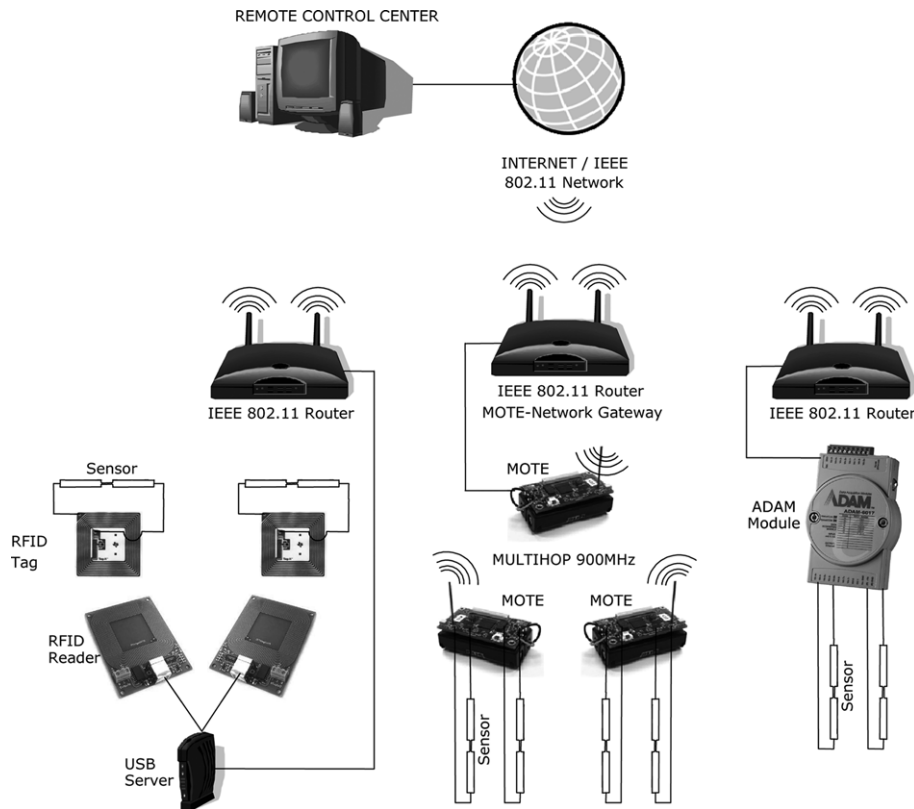


Fig. 12 Entire monitoring system

low-end RFID reader does. In the case of the mote, however, it is straightforward to use one mote and acquisition board to support multiple sensors, as illustrated in Fig. 11. For our hardware setup that allows up to 8 sensors for each mote/board, the cost per sensor is approximately \$40.

4.3 Data acquisition using an ADAM-6017 module

We have also experimented with an ADAM-6017 data acquisition module with eight 16-bit analog input channels (Advantech 2009). The ADAM-6017 module connects to a set of sensors as the MDA320CA board does and serves a similar purpose. The module requires a 2W unregulated DC power supply (leading to a total cost of approximately \$40 per channel) while the mote supporting the MDA320CA can be powered with AA batteries. Compared with the MDA320CA, the ADAM-6017 provides more stable sensing and has a built-in Ethernet port. We connect a Linksys 802.11 router to the Ethernet port in order to support wireless data communication (Fig. 12).

5. Data collection, processing and presentation

RSAN software runs at a remote control center and controls the sensors over either a local or wide-area network. The core of the RSAN software contains a collection of software objects, for

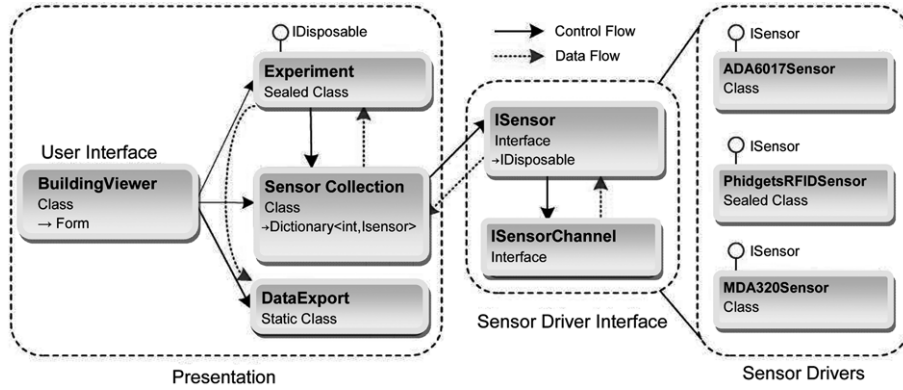


Fig. 13 Software architecture

essential sensor monitoring tasks including device and communication control and data collection, selection, logging and presentation. A sensor network deployment can be specified by configuring the objects as needed.

A configuration example is shown in Fig. 13. The configured objects “talk” to each other through well defined data and control ports; the directed lines in the figure show the data/control flows between these objects. The software architecture in Fig. 13 can be considered in three layers as shown: presentation, sensor driver interface and sensor drivers. Details on the software architecture are reported in Chin *et al.* 2008.

6. Experimental evaluation

6.1 Initial calibration

Thirty-seven sensors with $L_s=16$ in. were assembled for testing. They were calibrated by measuring the total deformation (between their ends) required to cause the rupture of the conducting copper strip for several lengths L_c (Fig. 8). Calibrations were made by attaching sensors with different gage lengths to two 2-in. diameter concrete cylinders, with each end of the sensor mounted on a different cylinder. One reinforcing steel bar was cast in each cylinder. The bars were used to mount the cylinders on a universal testing machine. With this machine, the cylinders were displaced with respect to one another at a constant speed. The total separation between the cylinders at the time of rupture was recorded. Rupture was detected using the simple setup shown in Fig. 14. In this setup, the data acquisition (DAQ) system registered a stable 9V signal before rupture. After rupture, the DAQ system registered a small floating voltage. The DAQ system was also used to record the elongation applied to the sensor. Lengths, L_c , ranged from 1/8 in. to 2.0 in. Fig. 15 shows a graph of the length L_c versus the deformation at rupture. This plot shows that the relationship between deformation and gage length is approximately linear. A relationship of this type can be used to determine the gage length required for the sensor to detect a given total deformation in the structural element. After we calibrated the prototype sensor described above, we used it to detect cracks on a column tested under constant axial load and cyclic lateral loads at the Nagoya Institute of Technology in Nagoya (NIT), Japan (Fig. 16). Two of the four vertical faces of this specimen were instrumented

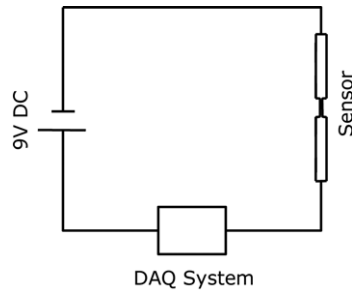


Fig. 14 Setup used for initial calibration of sensors

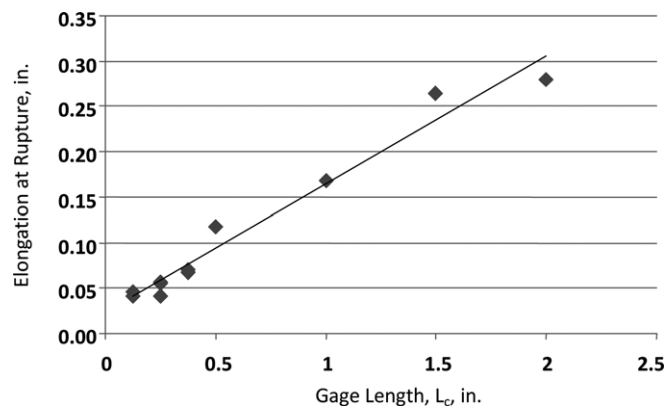


Fig. 15 Data used to calibrate prototype sensors



Fig. 16 Test specimen

with four sensors each: two with a 1/8-in. gage length and two with a 3/8-in. gage length. The locations of the two types of sensors used were alternated along each face.

The sensors were oriented as shown in Fig. 16 (perpendicular to the longitudinal axis of the column). This orientation enables the sensors to detect cracks forming at an angle with respect to the longitudinal axis of the column. This type of cracking has been observed repeatedly to lead to structural failures during past earthquakes.

Table 1 Measured and expected total crack widths

Sensor	L_c	Deformation at end of test or rupture		Rupture?
ID	(in.)	Expected (in.)	Measured (in.)	
1	1/8	0.05	0.05	Y
2	1/8	0.05	0.05	Y
3	3/8	0.07	0.08	Y
4	3/8	0.07	0.07	Y
5	1/8	0.05	0.05	Y
6	1/8	0.05	0.06	Y
7	3/8	0.07	0.07	N
8	3/8	0.07	0.08	N

6.2 Test results

Crack widths were measured with a crack-width comparator. During the test, six of the eight sensors detected deformations large enough to cause rupture of the sensor. The sensors with a length of 1/8 in. were expected to rupture, in average, at a total deformation of 0.05 in. The sensors with a length of 3/8 in. were expected to rupture at a total deformation of 0.07 in. Table 1 lists the observed total width of cracks that crossed each sensor. The mean of the measured crack widths matched the expected deformations at rupture.

6.3 Full-scale experiment

We also evaluated the performance of our structural assessment network using the full-scale three-story reinforced concrete building structure shown in Fig. 17. The structure was built by a team of researchers at Purdue University (Damon 2008) to investigate the response of flat-plate structures to earthquakes.

Each floor of the building measured 50 ft. by 30 ft. in plan. The total height of the structure was 30 ft. Six reinforced concrete columns, 18×18-in. in cross section, supported a total of three 7-in. thick flat slabs. The floor plan is shown in Fig. 18. The structure was subjected to 12 psf of

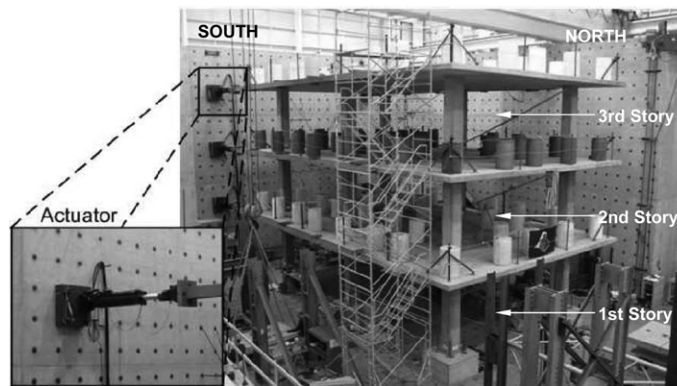


Fig. 17 Full-scale three-story test structure

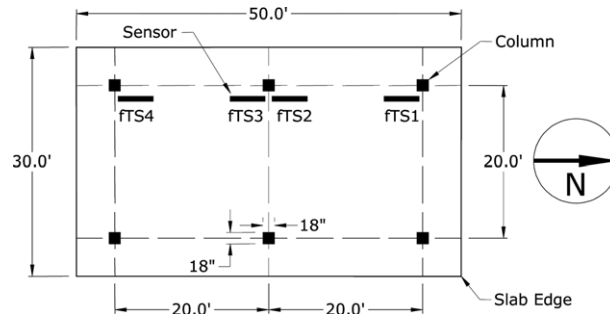


Fig. 18 Location of crack-width sensors

superimposed dead load applied with water-filled barrels. Cyclic lateral loads were applied with hydraulic actuators controlling the displacement at the top slab. Loads at the other two levels were adjusted to $2/3$ (at the floor of the third story) and $1/3$ (at the floor of the second story) of the load applied at the top level. Four displacement cycles were applied to the structure with maximum roof drift ratios of 0.22, 0.45, 1.5 and 3%. The assessment network was tested during the first three cycles. After the third cycle, 10 out of the 12 sensors used had reached their limits of operation.

We placed a set of four sensors on each of the three floors (Fig. 18), for a total of 12 sensors, to monitor deformations around the columns on the west side of the structure. The sensors used had a gage length L_c of $1/8$ in. The deformation at rupture was expected to exceed $0.03''$ (with an average of $0.05''$, Fig. 15). Each sensor was identified by a set of alphanumeric characters as in fTSn, where f is the floor number, and n is the sensor number, with numbers assigned from North to South. In the test, all three network configurations in Fig. 12 were used: sensors ITS3 and ITS4 were connected to RFID tags; ITS1, ITS2, and 2TS1-2TS4 were connected to the mote network; and 3TS1-3TS4 were connected to the ADAM-6017 module.

As expected, cracks that developed during lateral cyclic loading were concentrated around the columns. Fig. 19 shows cracks with thickness exceeding 0.01 in. observed after completion of the third cycle. Of the 12 sensors installed, 9 ruptured. All ruptures took place during cycles leading to total deformations exceeding $0.03''$. Two sensors did not rupture (3TS1 and 3TS4). The maximum deformation of the sensors that did not fracture was $0.03''$. Sensor 2TS1 was damaged accidentally before the test.

Sensors mounted near the South face of a column (sensors 1 and 3) ruptured during application of

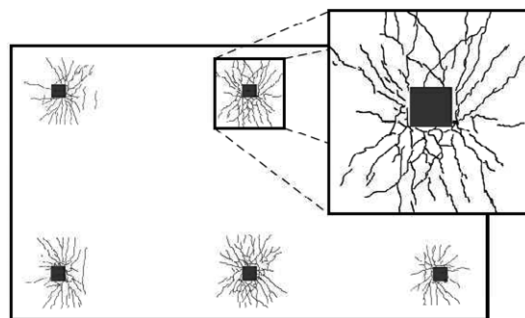


Fig. 19 Observed cracks (plan view)

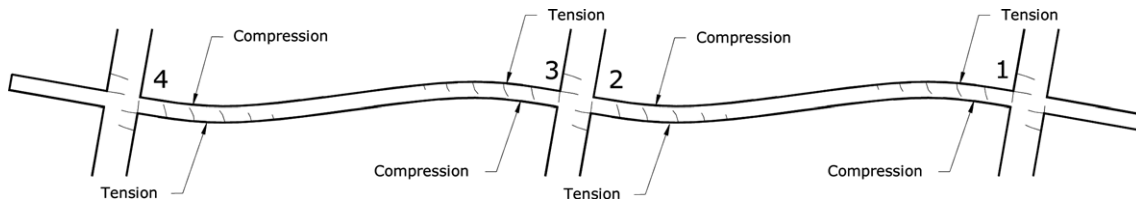


Fig. 20 Idealized deformed shape of slab

Table 2 Sequence of sensor ruptures

Cycle	Roof drift ratio	Load direction	Sensor/Total Width of Cracks (in. $\times 1000$)											
			1TS				2TS				3TS			
			1	2	3	4	1	2	3	4	1	2	3	4
1	0.22%	N												
1	-0.22%	S												
2	0.45%	N												
2	-0.45%	S												
3	0.90%	N	X		X				X					
3	1.50%	N											X	
3	-0.90%	S		X						X		X		
3	-1.50%	S				X		X						

The Xs indicate the cycles during which sensors were observed to have ruptured.

northward loads, while sensors mounted near the North face of a column (sensors 2 and 4) ruptured during application of southward loads. This observation is in agreement with the expected deformed shape (Fig. 20) and distribution of bending moments. Table 2 shows the observed sequence of ruptures.

6.4 Network results

For RFID, the status of a sensor was not updated periodically. Instead, an event was reported only when a tag was detected or communication with a previously detected tag was lost. The network reported the “loss of a tag” each time a sensor ruptured. We also observed occasionally very brief reports of the loss of a tag which did not correspond to rupture of a sensor. These “blips” were not expected. They are attributed to noise in the operating environment. Besides a very low rate of occurrence, the short duration of these “blips” has allowed us to separate the false from the true reports related to actual ruptures of sensors identified by permanent loss of communication with tags.

For the ADAM-6017, the control center polled the status of all eight channels of a data acquisition module (even if some of the channels were not connected to a sensor) once every second. Fig. 21 gives a representative trace of the data reports for one of the sensors connected to the ADAM-6017. Notice that there were two “blips” showing a 0.7 V and 0.2 V drops each lasting shorter than one second. The rupture of a sensor was associated with a large drop in the measured voltage as indicated in Fig. 21. Although the circuit design would have us expect zero voltage output after sensor rupture, the final voltage was not zero but fluctuated from 1 to 2 V. The large and permanent voltage

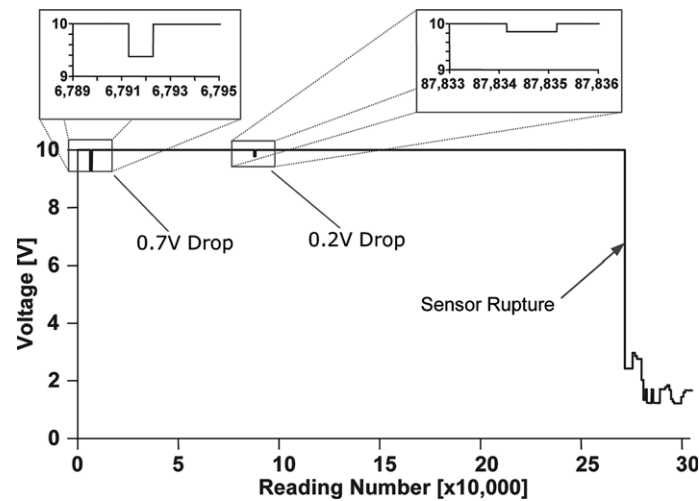


Fig. 21 Representative sample of recordings made with the ADAM-6017

drop after rupture of a sensor broke has allowed us to detect the rupture confidently.

For the MDA320CA/mote setup, the mote reports the status of all its data channels (for a data size of 36 bytes) at 0.5 Hz. The expected signal for a functional sensor was 2.5 V. But the network reported a sequence of 2.5-V readings, with periodic occurrences of 0.29-V readings at a frequency of about 1 in 58 readings. This noise was removed by computing a moving average of the readings.

6.5 Comparison of platforms used

All the platforms used can produce monitoring networks with low costs per sensor (from \$40 to \$75). The cost can be reduced if the supporting devices are replaced with devices with direct Wi-Fi access. For example, the existing Keyspan USB server and the ADAM-6017 provide only an Ethernet port, which required the use additional Linksys routers, at an extra cost, to bridge from Ethernet to Wi-Fi.

The use of RFID tags offers the possibility of monitoring sensors with hand-held readers, which would reduce both the cost of hardware and the required electric power. In this sense, the RFID platform appears to be the most versatile of the platforms used. However, in terms of the stability of the signals obtained, the platform based on the ADAM-6017 module appeared to be more robust, showing fewer and smaller fluctuations attributable to noise.

The group of sensing platforms investigated is by no means exhaustive. There may be better ways to achieve the results we have achieved. Our work has focused on testing and idea rather than implementing an optimal sensing system. The idea tested is that trying to detect structural damage directly may be easier and more useful than trying to infer damage from indirect measurements of stiffness or drift ratio (as discussed for the Holiday Inn Building). What constitutes damage is open for debate. But the symptoms of the possibility of collapse do not usually require such a debate (Fig. 22). In the case of the Holiday Inn Building, a wide range of crack-width sensors would have been adequate to alert a control center of the need for action.



Fig. 22 Column of holiday inn building (Faison *et al.* (2004))

7. Conclusions

The following remarks are made with the qualification that the proposed sensor system has not been tested under actual field conditions. It has been checked using test specimens and a full-scale three-story test structure in the laboratory where the accuracy of measurement and reliability of operation were uniformly positive.

The proposed sensors and the associated network promise to serve as a rapid structural assessment network for confident identification of structural failures in reinforced concrete construction. The sensors were successful in identifying cracks of predetermined size. The network has a low installation cost, low data rate, and data-loss resilience.

The most important and useful feature of the proposed system is that it promises to produce a crisp and immediate answer to the question of critical damage in a reinforced concrete structure. Another positive feature of the system is that the data from the sensor can be transmitted instantly to many points where it can be evaluated.

Acknowledgments

The work reported in this paper has been supported by National Science Foundation Grant # CMS0443148. The writers are indebted to Dr. S.C. Liu, program director, for his patience and help. Dr. S. Morita of the Building Research Institute, Tsukuba, Japan, and Dr. T. Ichinose of Nagoya Institute of Technology, Nagoya, Japan, were very helpful in all stages of the work. Mr. Jeffrey M. Rautenberg, Graduate Student at Purdue University, carried out the work done at Nagoya. The network was conceived and implemented by Mr. J.C. Chin, Graduate Student, and Dr. D.K.Y. Yau of the Computer Science Department, Purdue University. Mr. Jeffrey M. Rautenberg, Mr. Matthew Murray, and Mr. Tyler Krahn, Students at Purdue University, fabricated, calibrated, installed, and monitored the sensors.

References

- Advantech (2009), <http://www.advantech.com/>, Official web site of Advantech. Co.
- Aoki, S., Fujino, Y. and Abe, M. (2003), "Intelligent bridge maintenance system using MEMS and network technology", *Proceedings of the SPIE Conference*, San Diego, CA.
- Chin, J.C., Rautenberg, J.M., Ma, C.Y.T., Pujol, S. and Yau, D.K.Y. (2008), "A low-cost, low-data-rate rapid structural assessment network", *Proceedings of the 5th IEEE International Conference on Mobile Ad-hoc and Sensor Systems*, Atlanta.
- Chung, H.-C., Enomoto, T., Shinozuka, M., Chou, P., Park, C., Yokoi, I. and Morishita, S. (2004), "Real-time visualization of structural response with wireless MEMS Sensors", *Proceedings of the 13th World Conference on Earthquake Engineering*, Vancouver, BC, Canada.
- Crossbow Technology (2009), <http://www.xbow.com>.
- Damon Fick (2008), *Testing and structural evaluation of a large-scale three-story flat plate*, Doctoral Dissertation, Purdue University, April.
- Department of Conservation, Division of Mines and Geology (CDMG)(1994), *Processed data for Van Nuys - 7-Story hotel from the Northridge earthquake of 17 January 1994*, Strong Motion Instrumentation Program, Sacramento, CA.
- Faison, H., Comartin, C.D. and Elwood, K. (2004), *Reinforced concrete moment frame buildings without seismic details*, Report 111, Earthquake Engineering Research Institute, Oakland, CA.
- Farrar, C.R., Allen, D.W., Ball, S., Masquelier, M.P. and Park, G. (2005), "Coupling sensing hardware with data interrogation software for structural health monitoring", *Proceedings of the 6th International Symposium on Dynamic Problems of Mechanics*, Ouro Preto, Brazil.
- Lynch, J.P., Law, K.H., Kiremidjian, A.S., Kenny, T.W., Carryer, E. and Patridge, A. (2001), "The design of a wireless sensing unit for structural health monitoring", *Proceedings of the 3rd International Workshop on Structural Health Monitoring*, Stanford, CA, September.
- Morita, K. and Noguchi, K. (2006), "Crack detection sensor using RFID-Tag and electrically conductive paint", *AIJ J. Technol. Des.*, (24).
- Phidgets (2008), <http://www.phidgets.com/>, Official web site of Phidgets Inc.
- Straser, E.G. and Kiremidjian, A.S. (1998), *A modular, wireless damage monitoring system for structures*, Technical Report 128, John A. Blume Earthquake Engineering Center, Stanford University, Palo Alto, CA.
- Wang, Y., Lynch, J.P. and Law, K.H. (2005), "Validation of an integrated network system for real-time wireless monitoring of civil structures", *Proceedings of the 5th International Workshop on Structural Health Monitoring*, Stanford, CA, September.
- Wood, S.L. and Neikirk, D.P. (2001), "Development of a passive sensor to detect cracks in welded steel construction", *US-Japan Joint Workshop and Third Grantees Meeting*, Seattle, Washington.
- Zhao, F. and Guibas, L. (2004), *Wireless Sensor Networks: An Information Processing Approach*, Morgan Kaufman, San Francisco, USA.